# Transient Analysis of Double Layer Metal-Gas-Dielectric-Metal DBD Cell

G.T. Alisoy. F. Hansu, B.B. Alagöz, and H.Z. Alisoy

*Abstract*— **The investigation of Dielectric Barrier Discharges (DBD) in the absence of breakdown has significance in the perspective of the technological processes based on discharge phenomena and high voltage techniques. This study carries out transient analyses for the temporal evolution of electrical field, space charge density, polarization current while charging experimental Metal-Gas-Dielectric-Metal (MGDM) DBD cell. For these proposes, a theoretical model based on current continuity and two-layer polarization mechanism is developed for the investigation of an experimental MGDM electrodes system. In the steady state, the model obeys energy conservation law. Analysis results are discussed on the basis of experimental current measurements to explain pulsed DBD current.**

*Index Terms*— **Dielectric Barrier Discharge (DBD), MGDM system, Townsend Mechanism.**

## INTRODUCTION

IN RECENT years, much attention has been paid to non-thermal plasma due to its widespread use in many fields, such as, surface modifications, lamps, plasma displays, lasers, ozone generation, environment protection, biomedical applications and particle sources [1]. According to the driving frequency of power supply, non-thermal plasma can be generated by direct current (DC), alternating current (AC), radio frequency (RF) and microwave (MW) discharges [2]. Contrary to discharges caused from RF and MW, the electrode system is an important part in DC and AC discharges because the different shapes, materials and arrangements of electrodes have an effect on gas discharges [3-7].

The DBD is commonly used in surface treatment. Therefore, DBD increases local densities of charged particles near the surface, this result in increase of surface energy and

**G.T. ALİSOY,** Namık Kemal University, Department of Mathematics, Tekirdag, Turkey (e-mail: galisoy@nku.edu.tr)

**F. HANSU,** is with the Siirt University, Department of Electrical- Electronics, Malatya, Turkey (e-mail: f_hansu@siirt.edu.tr)

**B.B. ALAGÖZ,** is with the Inonu University, Department of Electrical-Electronics, Malatya, Turkey (e-mail: baykant.alagoz@inonu.edu.tr)

**H.Z. ALİSOY**, is with Namık Kemal University, Department of Electronics and Telecomunication, Tekirdag, Turkey (e-mail: halisoy@nku.edu.tr).

adhesion phenomena. Particularly, low-temperature gas discharge (corona, partial, glow, DBD) in electronegative gas media has been widely utilized in the modification of adhesion properties of dielectric polymers [8]. Incorporation of polar surface groups increases the surface energy and enable to cleaning or surface roughening. Furthermore, cross-linking and the formation of double bonds by chemically non-reactive species lead to surface stabilization [9]. In general, the increase in the surface energy of dielectric materials placed in electronegative gas media is explained by two mechanisms: (i) Chemical activation of the surface (the formation of free radicals on the surface) [10]. (ii) Free electrons, which are detached from negative ions, diffuse to the dielectric surface from the gas discharge region. These electrons are captured in the trap energy levels of the structure of dielectric material and as a result the electrets state form occurs [11, 12, 13]. In the MGDM electrodes systems, the charge accumulation between dielectric layers causes transient absorption and polarization currents. Measurements of these current and analysis of current characteristics have significance for the evaluation of high-voltage insulators [14]. Recently, nano-material fabrication technology benefits from dielectric barrier discharge plasma generators [15].

Another promising application of DBD is the plasma actuators developed for aerodynamic flow control [16, 17]. There are research efforts for possible use of plasma actuators in aerospace [18] and acoustic application [19]. These application uses asymmetric electrode placement to control ionic winds. Calculation of energy consumed by DBD system is an important parameter for application point of view, because the power of the system is strongly depended on the energy consumed in DBD processes. Removal of surface charge can improve flow controllability of DBD plasma actuator. Hence, electrical conduction mechanisms and charging kinetics of the DBD system are important for development of DBD applications. Honga et al. suggest an experimental method to measure surface charging of plasma actuators [20]. Several numerical simulation methods were proposed for simulation of DBD [21, 22, 23] and ionic flows [24]. However, a straight forward analytical modeling involving electro-physical mechanisms of DBD system is needed for analysis of electrical characteristic of DBD cells.

This study presents transient analyses for theoretical investigation of evolution of electrical field, free and relative charge density, current and energy-balance states for MGDM

DBD cell models. The developed theoretical model is based on the conductivity and polarization mechanism occurred in the gap of MGDM DBD electrodes system. Experimental measurements are conducted for symmetric and circular geometry of MGDM electrodes systems composed of polyimide dielectric barrier in the gas gap. The experimental results are interpreted on the basis of analytical modeling for the case that gap voltage is lower than breakdown voltage, $|U_g| < U_{br}$, in the absence of a breakdown. In this case it can be said that diffusion and polarization mechanisms are effective in conduction of dielectric barriers. The roles of these mechanisms in Pulsed DBD currents are also discussed.

Theoretical analysis addresses the following substantial issues in order to explain charging kinetics of DBD cells made of symmetric MGDM electrodes system:

(i) Transient analysis of electrical field evolution between the dielectric layers of DBD.

(ii) Investigation of free and relative space charges between surfaces of dielectric layers.

(iii) Transient current analysis in DBD cells.

(iv) Determination of energy consumed on MGDM systems and validation of the energy balance in DBD system.

## METHODOLOGY

### A. Experimental Study for Metal-Gas-Dielectric-Metal DBD System

Fig. 1(a) depicts MGDM electrodes while DBD is taking place. The schematic diagram of symmetric and circular geometry of MGDM electrodes system is illustrated in Fig. 1(b). The electrical schema of experimental setup is shown in Fig. 2. This experimental setup includes adjustable low-voltage power supply, electrical noise filter, high-voltage transformer, discharge chamber and measurement apparatus. The low-voltage system consists of a coupled transformer, filter and adjustable power supply. It provides an AC voltage adjustable in the range from 0 V to 220 V. The high-voltage transformer (TR3) generates an AC voltage in the range from 0 V to 33 kV. Discharge chamber includes electrodes system and safety cover. The electrodes system is composed of two electrodes and a polyimide dielectric barrier layer in an air gap.
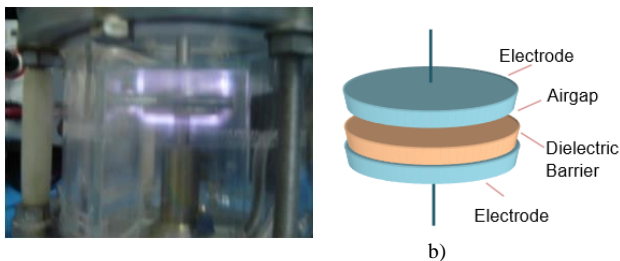


Fig.1. (a) Pictures of DBD taken place in the MGDM electrodes system (b) Schematic diagram of MGDM electrodes.
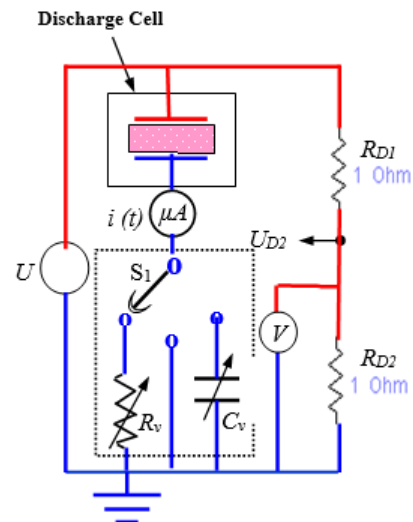


Fig.2. The experimental setup of DBD system

The DBD takes place between the two parallel plane electrodes. Both the upper and the lower electrodes are in shape of a steel cylinder and their thickness is 5 mm and the diameter is 25 mm. The dielectric barrier is made of a polyimide material film with thickness of 0.5 mm. The air gap is configured to 0.5 mm wide. The experiment was conducted in a static system in air at ambient temperature. The voltage applied to the electrodes is measured by a high voltage probe (AC High Voltage probe CT6). The discharge current and transported charges are measured by placing a 50 kΩ resistor (Rv) and a 33 nF capacitor (Cv) between the bottom electrode and the ground. The light emission image is recorded by a digital camera (Sony Cyber-Shot DSC T90) which is mounted for taking the side view of the air gap discharge. Lissajous diagram is measured by digital oscilloscope (TDS1002, Tektronix).

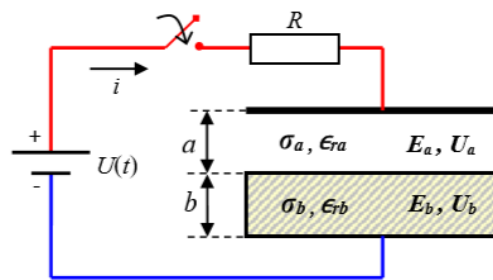### B. Transient Analyses of Experimental Metal-Gas-Dielectric-Metal DBD Process



Fig. 3. Schematic diagram of the experimental MGDM electrodes system.

Figure 3 shows schematic diagram of single barrier double layer MGDM electrodes system used in DBD cell. According to Kirchoff's second law, the following equation can be written:

$$iR + U_a + U_b = iR + E_a.a + E_b.b = U \qquad (1)$$

where the parameter a is the length of gas gap, Ea is the magnitude of electrical field in the gap and Ua denotes the voltage across the gap a. The parameter b is the thickness of polyimide dielectric layer, Eb is the electrical field in polyimide layer and Ub represents the voltage drop on the polyimide layer (dielectric barrier). The voltage of MGDM system is denoted by U. The electrical current flowing MGDM system is expressed as i=JS depending on the current density J and the area of the electrode S. Considering the static electrical field, the current density is commonly written as follow:

$$J = \sigma E + \varepsilon_r \varepsilon_0 \frac{dE}{dt} \qquad (2)$$

Considering current continuity condition Ja=Jb and Equation (2), the current density of MGDM system can be expressed as follow:

$$J_a = \sigma_a E_a + e_{ra} e_0 \frac{dE_a}{dt} = J_b = \sigma_b E_b + e_{rb} e_0 \frac{dE_b}{dt} \qquad (3)$$

where, $\sigma_a$ and $\sigma_b$ are conductance of gas gap and barrier layer, $\varepsilon_{ra}$ and $\varepsilon_{rb}$ are the dielectric constant of layers and Ja and Jb are the current densities, respectively. By considering almost zero conductivity due to assuming air gap an ideal dielectric layer $(\sigma_a \cong 0)$ during charging in the absence of breakdown, and using the Equation (1) and (3), the following two non-homogenous equations set can be obtained for the field evolution in two layer electrode systems,

$$\frac{dE_a}{dt} = -\frac{a}{RS\varepsilon_0 + e_{ra}} E_a - \frac{b}{RS\varepsilon_0 + e_{ra}} E_b + U$$
$$\qquad (4)$$
$$\frac{dE_b}{dt} = -\frac{a}{RS\varepsilon_0 + e_{rb}} E_a - \frac{(b + RS\sigma b)}{RS\varepsilon_0 + e_{rb}} E_b + U$$

By considering parameters of MGDM system, one can found the temporal evolution of electrical field given by Equation 5(a) and 5(b) by solving Equation (4),

$$E_a = E_{ak} + A_1 e^{p1}t + A_2 e^{p2t} \qquad (5a)$$

$$E_b = E_{bk} + B_1 e^{p1}t + B_2 e^{p2t} \qquad (5b)$$

In Equation (5), E$_{ak}$ and E$_{bk}$ parameters show steady state magnitudes of electrical fields in the layers. The parameters p1 and p2 are the Eigen values of the Equation (4). (See Appendix for the solution of the Eigen values) The parameters A1, A2, B1 and B2 are integration constants calculated depending on the initial conditions. Due to almost zero conductivity of ideal dielectric layer $(\sigma_a \cong 0)$ due the condition $|U_g| < U_{br}$, the conductivity currents flowing from

the gap layer of DBD cell model also becomes zero. Therefore, one can be written as the following:

$$E_{ak}.E_{bk}.b = U \qquad (6)$$

Since the polyimide material film has a0 conductivity greater than zero ($\sigma_b = 10^{-10} S \cdot cm^{-1} > 0$), the field intensity inside polyimide barrier is taken $E_{bk} \cong 0$. In this case, the electrical field in the gas gap of our experimental DBD cell can be calculated approximately as,

$$E_{ak} \cong \frac{U}{a} = \frac{1}{0.05} = 20 \frac{kV}{cm} \qquad (7)$$

When the initial conditions are taken as $U_a(0) = U_b(0) = 0$ and considering the parameters of experimental MGDM system ($a = 500 \ \mu m$, $b = 12.7 \ \mu m$ and $S = 4.9 \ cm^2$ in circular shape) and applied voltages ($U = 1 \ kV$), the overall system current and the current densities for the experimental system is calculated as:

$$i(0) = \frac{U}{R} = \frac{10^3}{103.10^3} = 9,71 mA \qquad (8a)$$

$$Ja(0) = Jb(0) = \frac{i(0)}{S} = \frac{9,71}{4,9} = 1,98 \frac{mA}{cm^2} \qquad (8b)$$

Considering these current densities, the electrical field of the experimental DBD system at $t = 0$ second can be estimated for $\varepsilon_{ra} = 1$ and $\varepsilon_{rb} = 3.56$ as,

$$\frac{dE_a}{dt}\bigg|_{t=0} = \frac{J_a(0)}{\varepsilon_{ra}\varepsilon_0} = 22,372.10^9 \frac{V}{cm.s} \qquad (9a)$$

$$\frac{dE_b}{dt}\bigg|_{t=0} = \frac{J_b(0)}{\varepsilon_{rb}\varepsilon_0} = 6,2845.10^9 \frac{V}{cm.s} \qquad (9b)$$

If initial conditions 9(a), 9(b) and $E_a(0) = E_b(0) = 0$ are used in Equation (5), magnitudes of electric fields in the layers of the MGDM system can be calculated as,

$$E_a(t) = 1,724.10^4 - 291 e^{-7,87.10^3 t} - 19,71.10^3 e^{-1135.10^3 t} \qquad (10a)$$

$$E_b(t) = 5,5756.10^3 e^{-7,87.10^3 t} - 5,5756.10^3 e^{-1135.10^3 t} \qquad (10b)$$

Under the condition of $|U_g| < U_{br}$, the relative and free charge densities collected at interface of layers can be expressed as,

$$q_s(t) = D_b(t) - D_a(t) \qquad (11a)$$

$$q_s^{relative}(t) = P_a(t) - P_b(t) \tag{11b}$$

where, Da, Db, Pa and Pb parameters are the displacement flux vectors and polarization vectors of the MGDM system for the air gap and the polyimide barrier layers, respectively. These parameters can be calculated as follow:

$$D_a(t) = \varepsilon_0 \varepsilon_{ra} E_a(t) \tag{12a}$$

$$D_b(t) = \varepsilon_0 \varepsilon_{rb} E_b(t) \tag{12b}$$

$$P_a(t) = \varepsilon_0(\varepsilon_{ra} - 1)E_a(t) \tag{12c}$$

$$P_b(t) = \varepsilon_0(\varepsilon_{rb} - 1)E_b(t) \tag{12d}$$

The electrical field solutions given by Equation 10(a) and (b) are used in Equation 11(a) and 11(b), the characteristics of free and relative electrical charges collected between gas and polyimide layers can be expressed as follow:

$$P_s(t) = 88,5.(20,14.e^{-7,87.10^3 t} - 0,141.e^{-1135.10^3 t} - 20)\frac{pC}{cm^2} \tag{13a}$$

$$q_{sr}(t) = 1,26.(e^{-7,87.10^3 t} - .e^{-1135.10^3 t} - 20)\frac{nC}{cm^2} \tag{13b}$$

The current of MGDM system depending on the differential of electro-physical parameters of MGDM system can be obtained as:

$$i(t) = \varepsilon_{ra}\varepsilon_0 S \frac{dE_a(t)}{dt} = \sigma_b S E_b(t) + \varepsilon_{rb}\varepsilon_0 S \frac{dE_b(t)}{dt} \tag{14}$$

$$= 0,009 e^{-7,87.10^3 t} + 9,7 e^{-1135.10^3 t} mA$$

Besides, in MGDM systems under condition of $|U_g| < U_{br}$, by taking into account the Equations 8(a)-(b), Equations 10(a)-(b) and Equation 14, energy-balance state analyses of MGDM system can be given as:

The source energy,

$$Ws = \int_0^\infty Ui(t)dt = 10^3 \int_0^\infty (0,009 e^{-7,87.10^3 t} + 9,7 e^{-7,87.10^3 t})dt = 9,68\mu J \tag{15a}$$

The energy consumed in resistance,

$$WR = \int_0^\infty Ri^2(t)dt = 103.10^3 \int_0^\infty (0,009 e^{-7,87.10^3 t} + 9,7 e^{-7,87.10^3 t})^2 dt = 4,807\mu J \tag{15b}$$

The energy consumed in ideal dielectric (air gap) layer,

$$W_G = E_{ak}, D_{ak}.S.\frac{a}{2} = \varepsilon_{ra}\varepsilon_0 E_{ak}^2.S.\frac{a}{2} = 4,336\mu J \tag{15c}$$

The energy consumed in dielectric (polyimide) barrier layer,

$$W_D = \int_0^\infty \sigma E_b^2(t).S.b.dt \tag{15d}$$

$$= \sigma bS \int_0^\infty (5,5756.10^3 e^{-7,87.10^3 t} - 5,5756.10^3 e^{-1135.10^3 t})^2 dt = 0,536\mu J$$

The energy state analyses given by equations 15(a)-(d) demonstrate that the energy-balance equation WS=WR+WG+WD is valid and the energy is conserved in the experimental system. In other words, the energy delivered from the source is equal to the energy consumed in the MGDM system. This result validates the consistency of our analyses.

## RESULTS AND DISCUSSIONS

In the previous section, an analytical model of experimental MGDM system was derived for the transient analyses based on the electro-physical processes in absence of breakdowns ($|U_g| < U_{br}$).

Fig. 4 shows characteristics obtained from these analyses: Fig. 4(a) illustrates the evolution of electrical fields in the gap ($E_a$) and in the dielectric barrier (polyimide) layer ($E_a$) according to Eq. 10(a) and 10(b), when 1 kV DC voltage is applied at $t=0$ second. Electrical field reaches saturation at about 17 kV/cm in the gap and about 8 10-3 kV/cm in the dielectric barrier at. Such a high electrical field discontinuity between layers indicates an electrical charge accumulation at the interface between layers. The increase in the amount of free electrical charges as shown in Fig.4(b) confirms this charge collection phenomenon between layers. Increase of charge density on the surface of the dielectric barrier results in decrease of electrical field intensity from 5 kV/cm to 8 10-3 kV/cm. Fig.4(c) shows relative charge accumulation calculated according to the polarization vector discontinuity. Figure 4(d) shows the transient current characteristics calculated by Eq. (14). During the charge collection in the MGDM system, a sharp current pulse is drawn from the DC source. After the electrical fields in the layers reach the saturation level in 0.6 millisecond, the transient polarization currents decrease to levels of leakage currents. Therefore, the charge collection between layers slows down. In the preceding of charge accumulation on the surface of dielectric barrier, the magnitude of leakage currents is very small compared to transient polarization current. The leakage current is mainly caused from increase in the surface conductivity of the dielectric barrier depending on the surface charging of polyimide. The volume conductivity is practically ignorable compared to charged surface conductivity of polyimide due to deficiency of free charge inside the polyimide volume.

Surface connectivity and the corresponding leakage currents sharply increase as the surface charging polyimide barrier increases. Nonlinear surface connectivity mechanism behaves as if a switch controlled by the charge density and results in periodic charge and discharge current pulses.
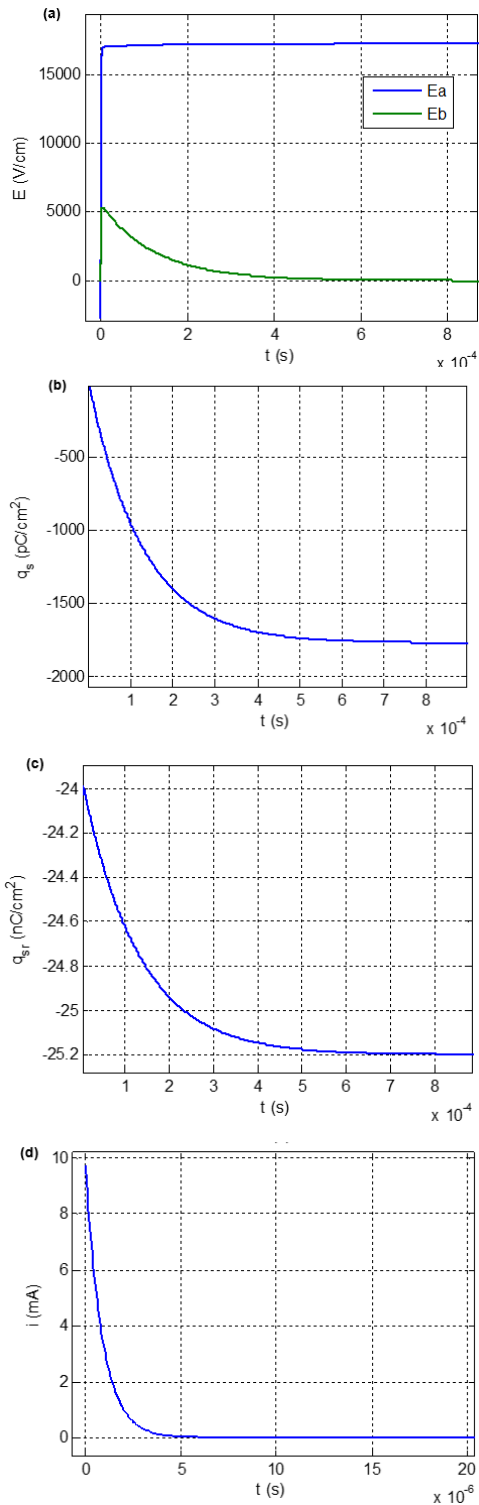
Fig. 4. Temproral evolution of electrical field intensities in layers (a), relative and free charge densities in (b) and (c), and the transient current in (d)

Fig.5(a) and 5 (b) compare measured currents from experimental setup and calculated transient current by using Equation (14). In Fig. 5 (b), transient periodical current was obtained by using the formula $i_p(t) = i(t) + i(t + n\Delta T)$, where parameter $\Delta T$ is the pulse period and $n = 1,2,3...$ The pulse period can determined from experimental measurements. Calculated

current array in Fig. 5(b) presents the consistency with the measured current pulse pattern in Figure 5 (a).

When equation (14) is considered, one observes two time constant parameters; $\tau_1 = 1/p_1 = 1.27 \, 10^{-4}$ second and $\tau_2 = 1/p_2 = 8.81 \, 10^{-7}$ second. The $\tau_2$ refers to the fast polarization of the air gap and the $\tau_1$ refers to the slower polarization of dielectric barrier as seen in Figure 4 (a). Polarization of dielectric barrier is mainly results from the ions precipitation on the dielectric surface from the air gap so that, at these field intensity levels, the dielectric barrier cannot generate free charges as much as the air gap.
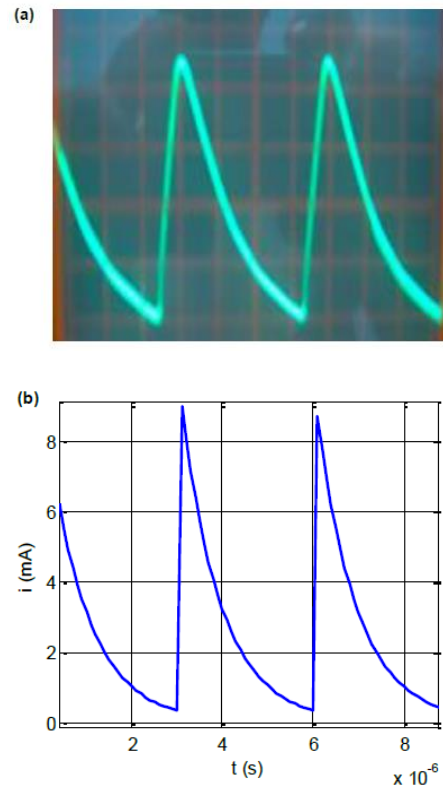


Fig. 5.(a) Experimental current of MGDM system (b) Calculated current pulse array.

Enough high electric field intensity in the narrow air gap can produce free ions due to ionization of gas molecules. These ions are accelerated by the electrical field and precipitates on the surfaces of dielectric barriers. The ions precipitations from gap result in the charging of dielectric barrier surfaces as represented in Figure 6 (a). The velocity of ionic flows determines effective depth of charge layer in the barrier surfaces. The surface charging also changes the activation energy of dielectric surface and this property is particularly useful for surface treatment applications. On the other hands, surface charging increases the surface conductivity of dielectric barriers and sharply increases leakage currents from the surfaces to the electrodes. These surface currents discharge the MGDM system and prepare it for the next charge-discharge session. This process repeats itself and results in periodic current pulses that are also known

as the Pulsed DBD (P-DBD) currents as shown in Figure 5 (a).

Subsequent charging-discharging processes of DBD are summarized by representation of the ion precipitation process in Figure 6. When the charge collection on the barrier surface reaches an adequate level, it stops further ion precipitation towards to the barrier surfaces for a while due to Coulomb force repelling free ions as in Figure 6 (b). Accordingly, a charge shield formed by Coulomb force appears near to the surface of dielectric barriers. The surface conductivity of the barriers sharply increases when charge accumulation reaches an adequate charge density on the surface. The resultant surface currents discharge the surface charges of the barrier and therefore it decreases Coulomb force to a level that initiates precipitation of the most recent charge layer as illustrated in Figure 6 (c). It increases again the surface charging of the barriers and delays ion precipitation, again. This process repeats itself and results in P-DBD currents corresponding to surface charge density of the barriers. Fundamentally, charge accumulation on the dielectric surface and the dependence of surface connectivity on charge density of the surface lead to appearing pulse trains on the measurement electrode of MGDM system.
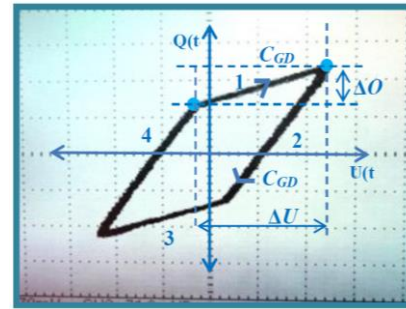


Fig. 7. Lissajous diagram of experimental MGDM system (measured by digital oscilloscope TDS1002, Tektronix)

This characteristic illustrates charging and discharging of the system for two opposite polarity of supply voltages. The figure indicates four capacitive region labeled by {1,2,3,4} according to the slope of curvatures. The charging capacitance ($C_{GD1}$) of MGDM system for positive voltage polarity can be calculated by the slope of line segment 1 as [25],

$$\Delta Q = C_{GD1} \Delta U \qquad (16)$$

where, $C_{GD1}$ is the charging total capacitance of MGDM system expressed as $C_{GD} = (C_D + C_G)$. $\Delta Q$ is measured from $C_v = 33\,nF$ measurement capacitance. (Vertical axis scaling is 71 mV and horizontal axis scaling is 408 V for oscilloscope screen in Figure 7) The experimental value of $C_{GD1}$ is calculated from Lissajous diagram as,

$$C_{GD1} = \Delta Q / \Delta U = 2.3\,10^{-9} / 1019 = 2.3\,pF \qquad (17)$$

Considering the increase of free charge density in Figure 4(d), one finds the deviation in charge density as $\Delta q_s = 1.76$ nC/cm2 while charging under the DC polarity voltage. Unit surface capacity of MGDM system can be obtained as,

$$c_{GD1} = \Delta q_s / \Delta U = 1.76\,10^{-9} / 1000 = 1.76\,pF / cm^2$$

Since, the area of the barrier layer is S=4,9cm2, the total capacity of MGDM system can be estimated as CGD=ScGD1=8,62pF. The theoretical total capacity is obtained at the level experimental value of CGD1, which is found 2.3 pF. This result shows that the analytical charging model is consistent with the experimental charging process of MGDM system for the operation region indicated the line segment 1 in the Coulomb-Volt characteristic. This confirms the relevance of theoretical calculations.

The slope of the line segment 2 yields the capacitance of MGDM system during discharge process when polarity of voltage is altered. The slope of the line segment 3 and 4 are corresponding charge and discharge capacitances for the opposite voltage polarities.
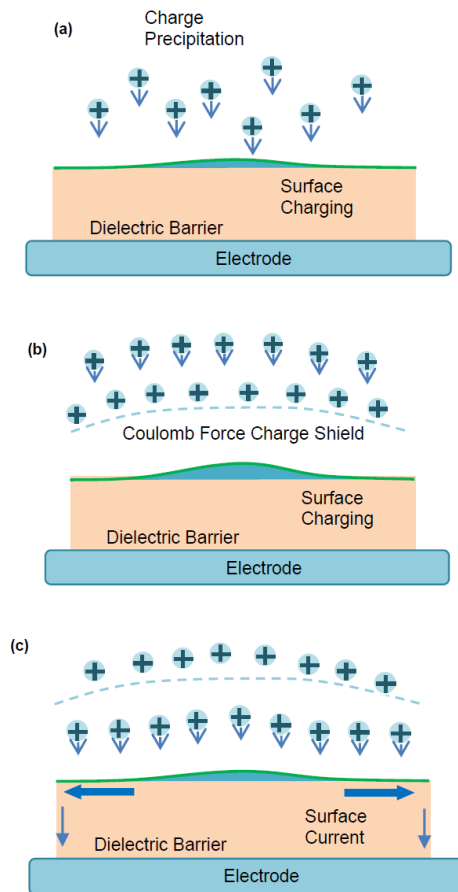


Fig. 6. A representation of charge layers on the surface.

Figure 7 shows Lissajous diagram of experimental MGDM system that shows Coulomb-Volt characteristic.

## CONCLUSION

A transient analysis of experimental MGDM electrodes systems was carried for the investigation of DBD phenomenon. The purposed analytical model, based on multilayer polarization mechanisms taking place inside MGDM system, conforms to the current continuity and energy conservation laws. The calculated current waveforms are in consistency with experimental transient current measurements. The energy delivered from the source was found equal to the energy consumed in the MGDM system. The energy balance state of analytical solution confirms consistency of the model.

The analyses and experiment results are useful for explaining physical mechanism involving in DBD phenomena. In the case of multilayer systems such as MGDM electrodes systems, charge collection between dielectric layers causes polarization of the system and lead to transient polarization current. However, increasing conductivity of dielectric barrier depending on surface charging leads to periodically polarization of system and therefore it results in P-DBD currents.

In practice, the measurement of these current and analysis of current characteristics provides useful information on the electrical properties of insulation systems. Alteration in properties of insulation system can be monitored by P-DBD current measurements. In order to enhance aerodynamic flow control performance of plasma actuators, surface charge removal from dielectric barrier may be needed. Because, Coulomb force charge shielding due high surface charge density may deteriorates controlling flow direction of ionic winds. It may be helpful to use barrier material that becomes conductive when surface charge density increases.

## APPENDIX

Equation (4) can be rearranged in the vector format as follows,

$$\begin{bmatrix} \dfrac{dE_a}{dt} \\ \dfrac{dE_b}{dt} \end{bmatrix} = \begin{bmatrix} k_{11} & k_{12} \\ k_{21} & k_{22} \end{bmatrix} \begin{bmatrix} E_a \\ E_b \end{bmatrix} + \begin{bmatrix} 1 \\ 1 \end{bmatrix} U \qquad (A1)$$

where,

$$k_{11} = -\frac{a}{RS\varepsilon_0\varepsilon_{ra}}, \ k_{12} = -\frac{b}{RS\varepsilon_0\varepsilon_{ra}}, \ k_{21} = -\frac{a}{RS\varepsilon_0\varepsilon_{rb}}, \ k_{22} = -\frac{(b+RS\sigma_b)}{RS\varepsilon_0\varepsilon_{rb}}$$

Characteristic equation of the differential equation system can be written as,

$$det\begin{bmatrix} k_{11}-p & k_{12} \\ k_{21} & k_{22}-p \end{bmatrix} = 0 \qquad (A2)$$

Then, one obtains following equation, $p^2 - (k_{11}+k_{22})p + k_{11}k_{22} - k_{12}k_{21} = 0$. By solving this equation, the Eigen values of Equation (A1) can be obtained as,

$$p_1 = \frac{(k_{11}+k_{22})}{2} + \sqrt{\frac{(k_{11}+k_{22})^2}{4} - (k_{11}k_{22} - k_{12}k_{21})},$$

$$p_1 = \frac{(k_{11}+k_{22})}{2} - \sqrt{\frac{(k_{11}+k_{22})^2}{4} - (k_{11}k_{22} - k_{12}k_{21})}.$$

## REFERENCES

[1] Bogaerts A., Neyts E., Gijbels R., Vander Mullen J. Gas discharge plasmas and their applications, Spectrochimica Acta Part B: Atomic Spect. Vol.57, pp.609-658 (2002).

[2] Napartovich A.P. Overview of atmospheric pressure discharges producing non-thermal plasma, Plasmas Polym. Vol.6, pp.1-14, (2001).

[3] Takaki K., Shimizu M., Mukaigawa S., Fujiwara T. Effect of electrode shape in dielectric barrier discharge plasma reactor for NOx removal, IEEE Trans. Plasma Sci. Vol.32 pp.32-38, (2004).

[4] Hepburn D.M., Kemp I.J., Richardson R.T., Shields A.J. Role of electrode material in partial discharge chemistry, Proceedings of the IEEE Fifth International Conference on Conduction and Breakdown in Solid Dielectrics, July 10–13 pp.605-610 (1995).

[5] Bhowmik S., Jana P., Chaki T.K., Ray S. Surface modification of PP under different electrodes of DC glow discharge and its physicochemical characteristics, Surf. Coat Technol. Vol.185 pp.81-91(2004).

[6] Dilecce G., Ambrico P.F., De Benedictis S. N2 density measurement in a dielectric barrier discharge in N2 and N2 with small O2 admixtures, Plasma Sources Sci. Technol. Vol.165, pp.11–522 (2007).

[7] Golubovskii Y.B., Maiorov V.A., Li P., Lindmayer M. Effect of the barrier material in a Townsend barrier discharge in nitrogen at atmospheric pressure, Journal of Phys. D: Appl. Phys. Vol.39, pp.1574-1583 (2006).

[8] Alisoy H.Z., Baysar A., Alisoy G.T. Physico-mathematical analysis of surface modification of polymers by glow discharge in SF6+N2 medium, Physica A: Statistical Mechanics and its Appl. Vol.351 pp.347–357 (2005).

[9] Massines F., Gouda G., A comparison of polypropylene-surface treatment by filamentary, homogeneous and glow discharges in helium at atmospheric pressure, Journal of Physics D: Applied Phys. 313, pp.411-3420 (1998).

[10] Amirov I.I., Izyumov M.O. Reactive ion etching of polymer films in an oxygen inductively coupled radiofrequency-discharge plasma, High Energy Chem. Vol.33,pp.119-123 (1999).

[11] Juvarly C.M., Aliyev (Alisoy) H.Z., Gorin Yu.V., Leonov P.V. On the role of the negative ions in the modification of the surface by electrical discharge, J. Surface Engineering and Applied Electrochem. Vol.138 pp.39-41 (1987).

[12] Juvarly C.M., Gorin Yu.V., Leonov P.V., Aliyev (Alisoy), H.Z. Process, Destruction and Stabilization of Polymer Materials, Proceedings of the Symposium on, IFRON, Dushanbe, 226 (1983).

[13] G.M. Sessler, Ed., Electrets, Berlin, Heidelberg, New York, (1980).

[14] Razevig D.V. High voltage engineering, Khanna Publishers, (1972).

[15] Bednara N., Matovićb J., Stojanovića G. Properties of surface dielectric barrier discharge plasma generator for fabrication of nano materials, J. Electrostat. Vol71 pp.1068–1075(2013).

[16] Kriegseis J., Möller B., Grundmann S., Tropea C., Capacitance and power consumption quantification of dielectric barrier discharge (DBD) plasma actuators, Capacitance and power consumption quantification of dielectric barrier discharge (DBD) plasma actuators, J. Electrostat. Vol. 69, pp.302–312 (2011).

[17] Roth J.R. Aerodynamic flow acceleration using paraelectric and peristaltic electrohydrodynamic effects of a one atmosphere uniform glow discharge plasma, Physics of Plasmas, Vol.10 pp.1166–1172 (2003).

[18] Shang J.S., Surzhikov S.T., Kimmel R., Gaitonde D., Menart J., Hayes J. Mechanisms of plasma actuators for hypersonic flow control, Progress in Aerospace Sci. Vol.41 pp.642–668 (2005).

[19] Li Y., Zhang X., Huang X. The Use of Plasma Actuators for Bluff Body Broadband Noise Control, Experiments in Fluids, Vol.49, pp.367–377 (2010).

[20] Honga D., Rabata H., Pub Y.K., Leroyc A. Measurement of the surface charging of a plasma actuator using surface DBD, Journal of Electrost. Vol.71 pp.547–550 (2013).

[21] Shkurenkov I.A., Mankelevich Y.A., Rakhimova T.V. Two-dimensional simulation of an atmospheric-pressure RF DBD in a H2 : O2 mixture: discharge structures and plasma chemistry, Plasma Sources Sci. Technol. 22 (2013) 015021.

[22] Hoskinson A.R., Hershkowitz N. Double DBD Plasma Actuator Simulations and Experiments in Quiescent Air, Plasma Science, IEEE 34th International Conference on, (2007).

[23] Flores-Fuentes A.A., Peña-Eguiluz R., López-Callejas R., Mercado-Cabrera A., Valencia A. R., Barocio S.R., Godoy-Cabrera O.G., Piedad-Beneitez A. de la, Benítez-Read J.S., Pacheco-Sotelo J.O., Modelling and simulation of a DBD plasma discharge supplied by a multicell inverter, In Proceedings of the 25th IASTED international conference on Modeling, identification, and control (MIC'06), M. H. Hamza (Ed.). ACTA Press, Anaheim, CA, USA, pp.249-254 (2006).

[24] Alisoy H.Z., Alagoz S., Alisoy G.T., Alagoz B.B., An Investigation of Ionic Flows in a Sphere-Plate Electrode Gap, Plasma Sci. Technol. Vol.15: pp.1012-1019 (2013).

[25] Kuchinskii G.S., Partial Discharge in High Voltage Constructions, L. Energy, 1979.

## BIOGRAPHIES

**GULIZAR ALISOY**, was graduated with honors from the Faculty of Mathematics and Mechanics of the Azerbaijan State University. Her M.Sc.(85') and Ph.D. (97').She received Assoc. Prof. degree in Analysis and Theory of functions from High Education Council of Turkey in 2012. Currently, she is Assoc.Professor, in Mathematical Department of Namik Kemal University. Her research interests are, integral representation of multi-package variable functions, differential properties of functions, mathematical modeling of engineering problems.

**FEVZI HANSU**, was graduated from University of Inonu, department of Electrical and Electronics Engineering in 2001. He worked for Kalyon Plastic and Man-Olp for several years. He is following Ph.D. at Inonu University department of Department of Electrical-Electronics Engineering. He has been working as an Asst. Prof. at the Siirt University, Department of Electrical and Electronics Engineering.

**BARIS BAYKANT ALAGOZ**, was graduated from University of Istanbul Technical University department of Electronics and Communication Engineering in 1998. He worked for Alcatel Microelectronics and Turkish Telecom for several years. He is following Ph.D. at Inonu University department of Department of Electrical-Electronics Engineering. He has been working as an Asst. Prof. at the Inonu University, Department of Electrical and Electronics Engineering.

**HAFIZ Z. ALİSOY,** was graduated from Moscow Technical University department of ElectroPhysics Engineering 1982. He had his PhD degree from USSR Science Academy Physics Institute of P.N. Lebedyev and Doctor of Sciences degree (DSc) from International Ecology-Energy Academy. He became as Full Professor in 1995. He received award of Young Scientist. He works at Namık Kemal University, Department of Electronics and Telecommunication Engineering.